

One-Equation Sub-Grid Scale (SGS) Modelling For Eulerian–Eulerian Large Eddy Simulation (EELES) of Two Phase Solvent Extraction Pump Mixer Unit.

Mandar Tabib and Philip Schwarz

CSIRO Mathematics Informatics and Statistics Division, Clayton, Victoria 3169, AUSTRALIA

Abstract

The pump mixers are widely used in a solvent extraction (SX) process. Any improvement in understanding of hydrodynamics and flow instabilities within a SX pump mixer unit would enable effective design of the mixer-settler equipment. In this direction, the present work investigates the predictive performance of the One-equation model for Sub-grid scale turbulent kinetic energy Large Eddy Simulation (1-Eqn. SGS-TKE LES model) vis-à-vis other LES models (Smagorinsky LES model, Dynamic LES model), the PIV experimental results and the RANS based model. Comparisons have been made initially for single phase operation of a pump-mixer unit, and then for the multiphase operation. The ANSYS/CFX modelling package has been used to set-up a transient three-dimensional CFD model using the sliding mesh approach for impeller motion and Eulerian-Eulerian approach for multi-phase flows. The 1-Eqn. SGS-TKE LES model has been implemented in CFX using user routines. The prediction of instantaneous flow structures and turbulence intensities using this model will pave the way for determination of droplet size and mass transfer rates, which are required in designing these systems. To the best of author’s knowledge, this is the first use of a transport equation for SGS kinetic energy in simulating two phase liquid-liquid flows.

Introduction

Solvent extraction based hydrometallurgy processes are widely used in copper, nickel, uranium and cobalt industries and are implemented through the use of Mixer-Settlers. A typical mixer settler set-up (as shown in Figure. 1A) involves a solvent extraction pump mixer (Figure. 1B), comprising of a mixing impeller, a false bottom for inlet of fluids and a weir at the top for discharge. The impeller on rotation creates a pressure drop or head that generates the flow, and creates a high shear region for droplet formation and break-up. The main design objective in the mixer section involves achieving a sufficiently small droplet size for mass transfer to take place, without generating a population of fine droplets that will be difficult to separate in the settler.

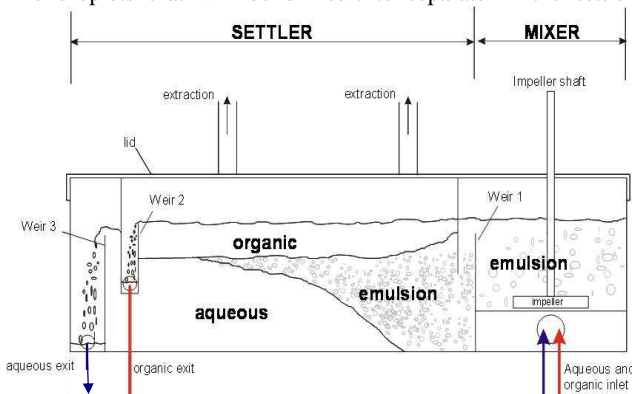


Figure 1A shows schematic diagram of geometry.

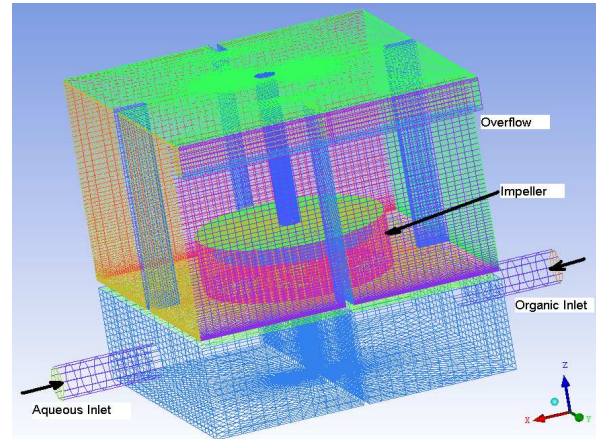


Figure 1B shows typical grid and directions used in this study.

Figure 1(A-B) shows schematic diagram of geometry.

One way of achieving this is through a proper understanding of hydrodynamics and turbulent conditions within the mixer unit, and this would require an advanced turbulence modelling approach. Recently, the Large Eddy Simulation (LES) turbulence model has shown significant promise in unearthing flow details in gas-liquid multiphase systems [3,7,10,11], and, in this work, we plan to use this for analysing liquid-liquid system.

Model Equations

The numerical simulations presented here are based on both a single phase model and a multiphase model. For space reasons, the multiphase model is described, which is a two-fluid model based on the Euler-Euler approach. The eulerian modelling framework is based on ensemble-averaged mass and momentum transport equations for each of these phases. These transport equations without mass transfer can be written as:

Continuity equation

$$\frac{\partial}{\partial t}(\rho_r \alpha_r) + \nabla \cdot (\rho_r \alpha_r \mathbf{u}_r) = 0 \quad (1)$$

Momentum transfer equations

$$\frac{\partial}{\partial t}(\rho_r \alpha_r \mathbf{u}_r) + \nabla \cdot (\rho_r \alpha_r \mathbf{u}_r \mathbf{u}_r) = -\nabla \cdot (\alpha_r \boldsymbol{\tau}_{ij,r}) - \alpha_r \nabla P + \alpha_r \rho_r \mathbf{g} + M_{F,r} \quad (2)$$

In this work, the phases are continuous aqueous phase ($r=a$) and dispersed organic phase ($r=o$). The variable (α_r) represents the volume-fraction of the respective phases. The terms on the right hand side of equation (2) are respectively representing the stress, the pressure gradient, gravity and the ensemble averaged momentum exchange between the phases, due to interfacial forces (like, drag force, lift force, virtual mass

force and turbulent dispersion force (TDF) respectively). For simulating liquid-liquid flow in pump-mixer, only the drag force and TDF are considered in this work. The drag coefficient for the drag force has been determined through the empirical correlations of Ishii and Zuber [5], and TDF contribution is based on incorporating SGS kinetic energy. The pressure is shared by both the phases. The stress term of phase r is described as follows:

$$\tau_{ij,r} = -(\mu_{l,r} + \mu_{t,r}) \left(\nabla \mathbf{u}_r + (\nabla \mathbf{u}_r)^T - \frac{2}{3} I(\nabla \cdot \mathbf{u}_r) \right) \quad (3)$$

where, $\mu_{l,r}$ and $\mu_{t,r}$ are laminar and turbulent viscosity respectively. The aqueous phase turbulent eddy viscosity ($\mu_{t,a}$) is formulated based upon the turbulence model used (k- ϵ turbulence model or LES turbulence model), and have been described below, while the effective organic dispersed phase viscosity is computed as:

$$\mu_{eff,o} = \left(\frac{\rho_a}{\rho_o} \right) \mu_{eff,a} \quad (4)$$

k- ϵ Turbulence Model

When the k- ϵ model is used, the velocities (\mathbf{u}) in continuity and momentum equations (equations 1-2) represent the time averaged velocities. The turbulent eddy viscosity is formulated as:

$$\mu_{t,a} = \rho_a C_\mu \frac{k^2}{\epsilon} \quad (5)$$

The turbulent kinetic energy (k) and its energy dissipation rate (ϵ) are calculated by solving governing transport equations.

LES Models

Equations for LES are derived by applying a filtering operation to the Navier-Stokes equations. The filtered equations are used to compute the dynamics of the large-scale structures, while the effect of the small scale turbulence is modelled using a SGS model. Thus, the entire flow field is decomposed into a large-scale or resolved component and a small-scale or sub-grid-scale component. In case of LES, the velocities (\mathbf{u}) in continuity equations and momentum equations (equation.1-2) represent the resolved velocities or grid scale velocities. The SGS stress modelling requires computation of a turbulent eddy viscosity, which is formulated depending upon the LES model selected. In this work, the Smagorinsky model [9], the dynamic Model [4,6] and 1-Eqn. SGS-TKE LES model [2,7] has been chosen.

Smagorinsky Constant Model

The Smagorinsky model [9] used the following expression to calculate the turbulent viscosity, i.e the SGS viscosity:

$$\mu_{t,a} = \rho_a (C_s \Delta)^2 |S|^2 \quad (6)$$

Where, C_s is the Smagorinsky constant, S is the strain rate and Δ is the filter width and it is computed based on the cell- grid-size, so, $\Delta = (\Delta_i \Delta_j \Delta_k)^{1/3}$, where, i, j and k are directions. The constant C_s is different for different flows. In the literature for single-phase flow, the constant is found to vary in the range from $C_s = 0.065$ to $C_s = 0.25$. For this work, a C_s value of 0.12 is taken.

Dynamic Smagorinsky Model

The uncertainty in specifying the constant C_s in Smagorinsky model led to the development of the dynamic sub-grid model in which the constant C_s is computed. The main idea here is to

introduce a filter $\{\Delta\}$, with larger width than the original one, i.e. $\{\Delta\} > \Delta$. This filter is applied to the filtered Navier-Stokes equations (the NS equations are filtered twice), yielding the value of C_s , which is used in equation (6). The second filter, usually called the test filter, which is twice the mesh size in the present study, has been applied to the velocity field.

One-equation SGS TKE LES Model

In this case, the eddy viscosity is calculated from:

$$\mu_{t,a} = \rho_a C_k \Delta k_{sgs}^{1/2} \quad (7)$$

Where, k_{sgs} represents the SGS kinetic energy, which is obtained by solving for transport equation for k_{sgs} .

$$\frac{\partial}{\partial t} (\rho_r \alpha_r k_{sgs}) + \nabla \cdot (\rho_r \alpha_r \mathbf{u}_r k_{sgs}) = -\nabla \cdot \left(\alpha_r \frac{\mu_{eff,r}}{\sigma_k} \nabla k_{sgs} \right) + \alpha_r \left(G_r - C_\epsilon \frac{k_{sgs}^{3/2}}{\Delta} \right) \quad (8)$$

Where, G is the production term, defined as:

$$G_r = \mu_{T,a} \left| S_{ij} \right| \quad (9)$$

The value of model constants ($C_\epsilon=1.05$ and $C_k=0.07$) in equation (8) are considered on the basis of recommendation by Davidson [2].

Modelling Details

Geometry

The pump mixer unit comprises of a square mixer box (of dimensions 450mmx450mmx450mm) equipped with a lightning R320 impeller (of diameter 230 mm and positioned about 5 mm above the false bottom). The mixer has been modelled with an impeller speed of 200 rpm (tip speed of 2.4 m/s). In this work, only the pump-mixer region has been simulated. There is a separate inlet section for the organic and aqueous phases located in the bottom section below, where they flow in at a rate of 15 l/min each. The outlet from the mixer box is in the form of an overflow via a weir to a rectangular settler (of dimensions 1410mm x 450mm).

Model Setup

The ANSYS/CFX modelling package has been used to set-up a transient three-dimensional CFD model using the sliding mesh approach for impeller motion and Euler-Euler approach for multi-phase flows. In this work, the interface separating the static and revolving mesh is mid-way between the impeller-tip and baffles, as has been suggested in the literature. The choice of interface location is critical given the close proximity of impeller tip and the baffles. For single phase, the aqueous phase inlet velocity is 30 l/min. For multi-phase, both aqueous phase (1000 kg/m³ density, 1 cp viscosity) and organic phase (930 kg/m³ density, 3 cp viscosity) enter through separate inlets at 15 l/min. The through-flow rate was determined based on a target residence time of 2 minutes in the mixer. The pump-mixer comprises of a R320 impeller revolving at 200 rpm. For k- ϵ model, the high-resolution scheme has been used and for LES, the central difference scheme has been used for spatial discretization of the advection terms. The second-order implicit scheme has been used for time discretization in both the cases. The LES run has been initialized with a perturbed RANS transient solution run to achieve steady flow (around 20 impeller rotations). For k- ϵ runs, the time-step has been the time taken by impeller to revolve by 15° (around 0.01 s) and for LES, it is around 8 x 10⁻⁴ s. The selected time-step ensures proper convergence and capture of transient flow structures. The

simulations were performed for a time-span of around 10 sec, which corresponds to around 33 revolutions of the impeller. For multiphase simulation, the average droplet diameter was taken as 0.6 mm, based on the results from experimental photographic techniques

Resolution Issues While Applying LES

The accuracy of LES simulations depends upon grid size and resolved kinetic energy. For accurate LES results, the modelled SGS stress should account for a negligible fraction of the total stress. In other words, the grid should be sufficiently fine so that only smaller, isotropic eddies are modelled. Baggett et al. [1] suggested that SGS stress becomes isotropic when filter width is a fraction of turbulent dissipation length scale (preferably, 0.1). This has been used in this work as the criteria to obtain an appropriate grid size. The turbulent dissipation length scale has been obtained from k and ϵ values of the $k-\epsilon$ model.

The volumetric average of ratio $(vol)^{1/3} / (k_a^{1.5} / \epsilon_a)$ is around 0.6. Thus, while the grid is a bit coarse, it can be regarded as suitable for moderately resolved LES simulations. The mesh consisted of 587000 cells (hexahedral elements) with relatively fine mesh near the impeller to better resolve the velocity fields. In pump mixers, the turbulent structures are generated by large and rotating geometrical features and flow curvature. Hence, the near wall spacing criteria is relaxed with use of appropriate wall functions. The other issue in LES is resolved kinetic energy. Pope [8] suggested that the ratio of resolved turbulent kinetic energy to the total turbulent kinetic energy $(k_r / (k_r + k_{SGS}))$ be used as a measure to analyse the adequacy of the fluid flow being resolved by LES. For a well-resolved flow, the ratio is greater than 80%. In this work the ratio is above 70% when averaged over the tank, and in regions with higher turbulence near the impeller and in the bulk, the ratio is greater than 80%. Thus, the results from this LES run can be considered to moderately resolved and acceptable for analysis.

Results For Single Phase Mixer
Time Averaged Profile

Figures 2 (A-E) shows qualitative predictions of velocity vectors as obtained by various models and can be compared to the PIV Experimental Data at a plane located at $x=-0.112$ m. In PIV snapshot (Figure. 2A), at the right side of impeller, the recirculating flow doesn't reach the top right side wall.

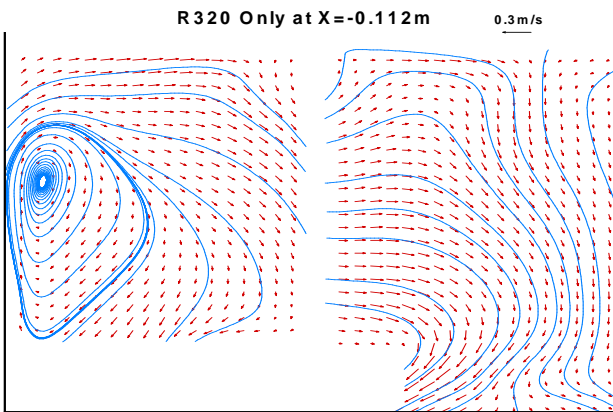


Figure 2A shows velocity vectors obtained from PIV.

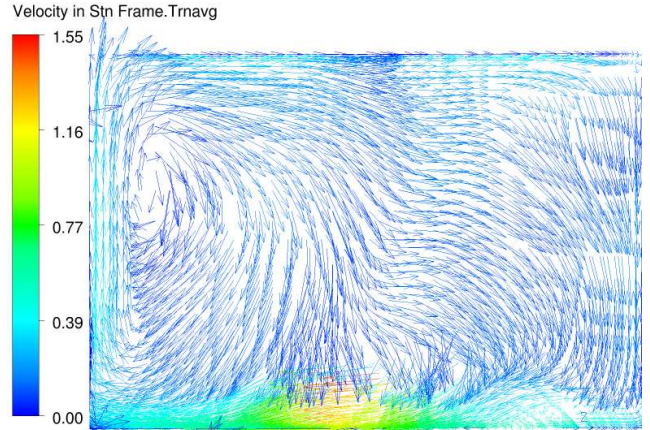


Figure 2B shows velocity vectors predicted by LES One equation model.

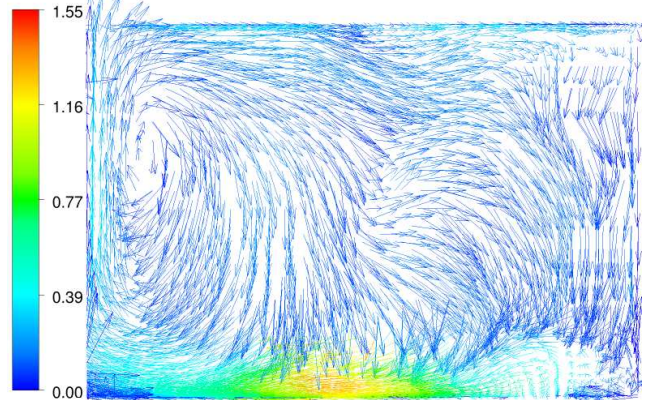


Figure 2C shows velocity vectors predicted by LES smagorinsky model.

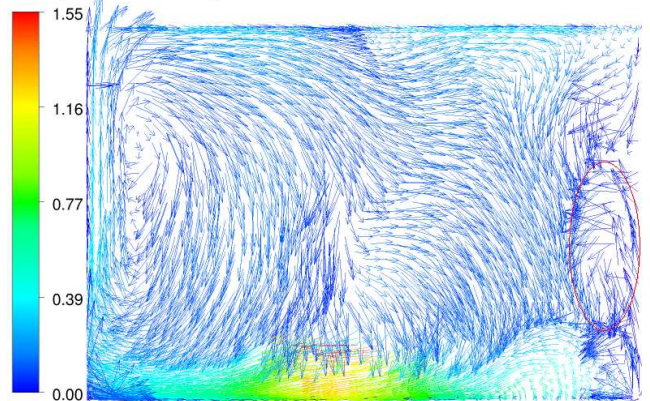


Figure 2D shows velocity vectors predicted by LES dynamic model.

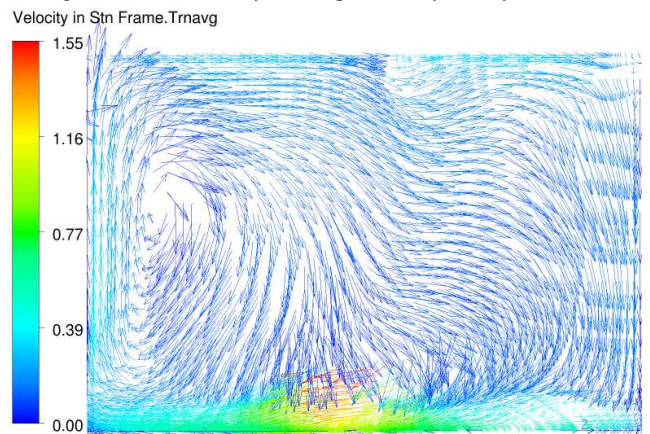


Figure 2E shows velocity vectors predicted by RANS model. Figure 2 (A-E) shows comparison of time averaged flow profile at $x=-0.112$ m location captured by various turbulence models and PIV (Velocities in m/s).

The 1-Eqn.SGS-TKE LES model and smagorinsky LES model (Figure. 2B and 2C) are closer to the flow pattern given by the PIV experiment. The Dynamic LES Model (Figure. 2D), on the other hand, deviates a bit from experimental observation by showing recirculation's of flow near the right wall (marked in red circles),while the RANS Model (Figure. 2E) shows one circulation covering the whole right side of impeller, here the recirculating flow reaches the right side wall.

Figure. 3 compares predicted values to experimental values of time averaged axial velocity along the y direction at location $x = -0.168$ m, $z = 0.323$ m for the pump-mixer operating with a single phase.

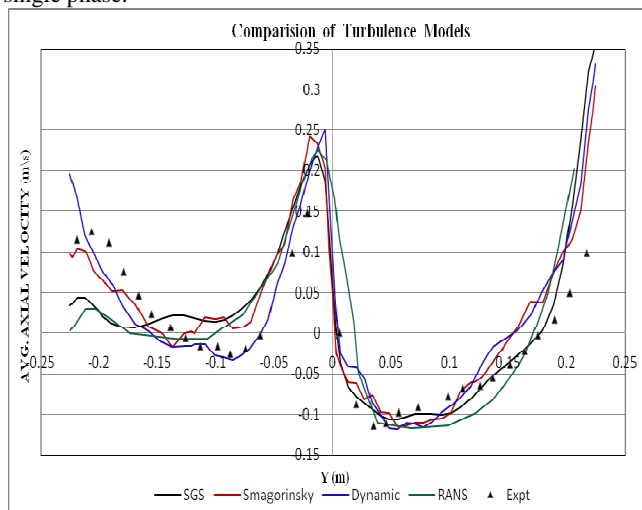


Figure 3 compares performance of turbulence models.

Figure. 3 reveals that most computational models deviate from the experiment at $y=0$, where they predict a higher positive axial velocity arising from a re-circulation. The deviation of the One-equation LES model is lesser than other LES model. Apart from that at other regions, the prediction is within fair agreement. The over-prediction of centre velocity is a result of the local eddy viscosity values computed by various models. This could be because the present LES model is moderately resolved.

Flow Pattern

Figure. 4 compares the mean flow profile obtained from the RANS model at a given time (Figure. 4A) with the instantaneous flow profile from 1-Eqn. SGS-TKE LES (in Figure. 4B). Velocity in Stn Frame

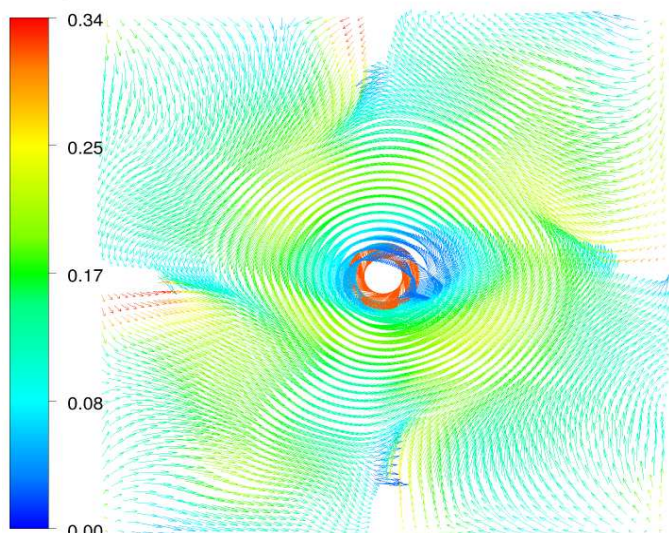


Figure 4A shows RANS model prediction of mean velocity at XY plane at $z=0.42$ m height.

Water.Velocity in Stn Frame

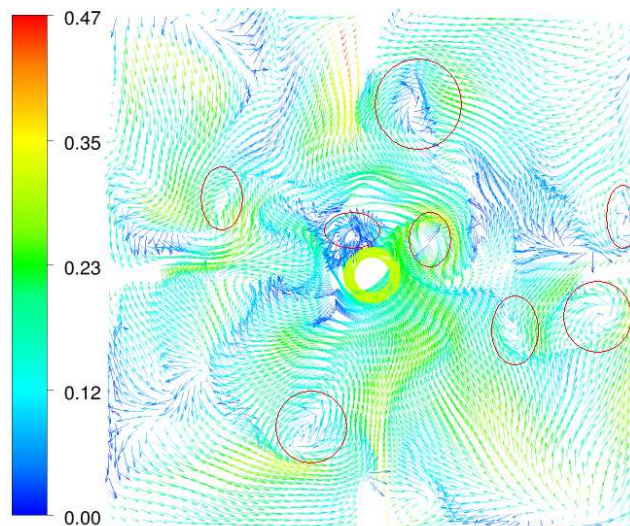


Figure 4B.LES prediction of instantaneous flow at XY plane at $z=0.42$ m height.

Figure 4 compares flow profiles by RANS and LES.

The RANS model results are limited to giving information on averaged profiles, while at the same plane, the instantaneous LES (Figure. 4B) is able to capture the chaos and turbulent eddies (marked in red in Figure. 4B). The 1-Eqn. SGS-TKE LES model is able to capture precession vortices near the rotating shaft.

Figure 5 shows the sub-grid scale turbulent kinetic energy predicted by 1-Eqn. SGS-TKE LES model. The 1-Eqn. SGS-TKE LES model is thus advantageous as compared to both the dynamic and smagorinsky model which cannot give the information on sub-grid scale energies. The information on SGS-TKE can be helpful in determining accurately the turbulent dispersion and obtaining accurate total kinetic energy. This paper has delved deeper into the issue of sub-grid scale dispersion effects. Hence, future work would involve obtaining more information using 1-Eqn. SGS TKE LES model. The information obtained from this would be useful in understanding effect of turbulence on droplet diameter and mass transfer rates at different regions.

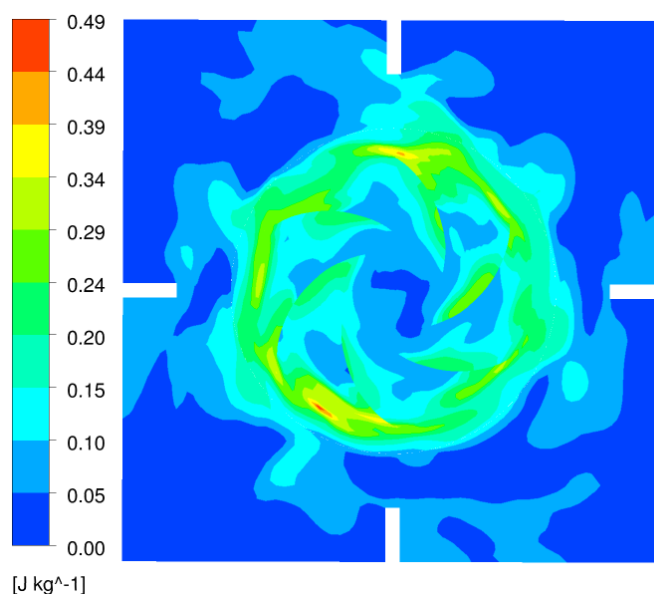


Figure 5. SGS turbulent kinetic energy predicted by One-equation model.

Instantaneous Profiles For Multi-phase Mixer

Figure. 6A shows the velocity profile obtained at a time step by the multi-phase RANS model. The RANS model shows only a gross circulation pattern and has not been able to resolve the detailed flow structures. Figure. 6B shows the instantaneous two phase hydrodynamics captured by 1-Eqn. SGS-TKE LES, with the organic kerosene phase entering the lower left and aqueous phase at lower right of the false bottom. Both phases get drawn up by the pump mixer, and dispersion of organic droplet phase and extraction happens in the pump-mixer box. The organic volume fraction is around 50-60% in the pump-mixer box, where it exists in fine droplet form after being sheared by the impeller. The LES models used have been able to capture the instantaneous flow structures (as marked in red in Figure. 6B).

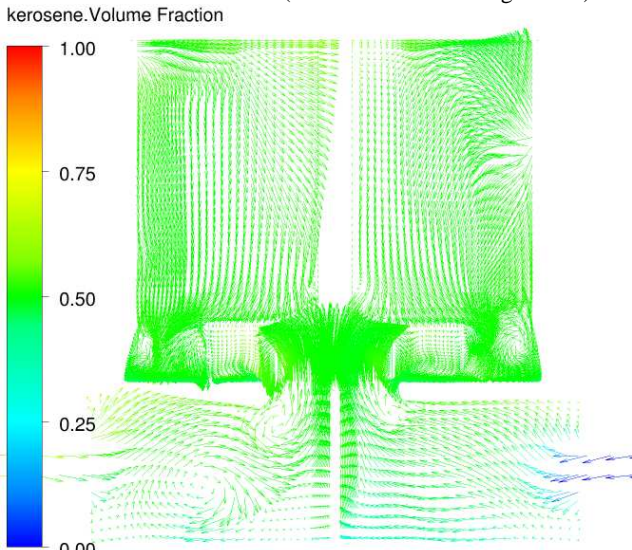


Figure 6A shows RANS prediction of mean velocity and dispersion.

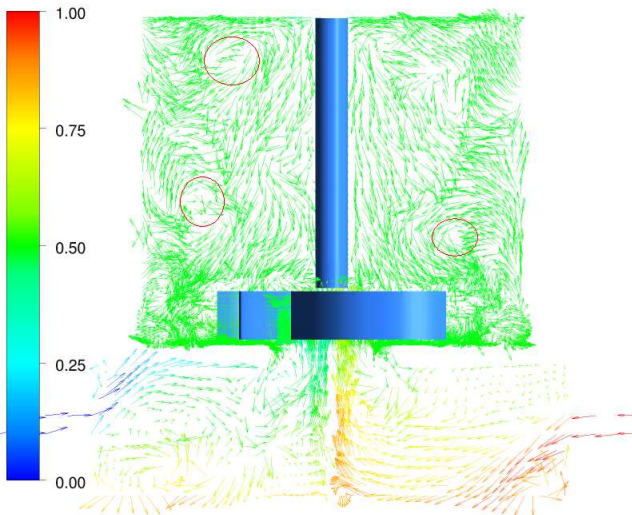


Figure 6B shows LES based instantaneous flow structures and dispersion.

Figure. 6(A-B) compares performance of LES and RANS in predicting flow and dispersion at $x=0$ m location.

Conclusions

The obtained results reveal that the One-equation SGS model gives comparative results to the well-established dynamic and smagorinsky model with the additional benefit of giving information on the modelled SGS energy. Introducing a one-equation model for the SGS kinetic energy, allows a better insight into the phenomena taking place at the SGS level. The

present work raises hope of being able to utilize the SGS information.

Acknowledgments

The authors of the paper would like to acknowledge CSIRO OCE funding to one of the authors. The experimental data used in this paper was obtained in the P706 project funded through AMIRA International. The authors would like to thank William Yang for performing the experiments and Graeme Lane for his inputs.

References

- [1] BAGGETT, J.S., JIMÉNEZ, J., & KRAVCHENKO, A.G., (1997), "Resolution requirements in large-eddy simulations of shear flows", Annual Research Briefs., Stanford Centre for Turbulence Research.
- [2] DAVIDSON, L., (1997). Large eddy simulations: a note on derivation of the equations for the subgrid turbulent kinetic energies. Technical Report No. 97/12, 980904, Chalmers University of Technology, Gothenburg, Sweden.
- [3] DEEN N., SOLBERG T. & HJERTAGER B., (2001), "Large eddy simulation of gas-liquid flow in a square cross-sectioned bubble column", Chemical Engineering Science, 56, 6341-6349.
- [4] GERMANO, M., PIOMELLI, U., MOIN, P. AND CABOT, W. H., (1991), "A dynamic subgrid-scale eddy viscosity model", Physics of Fluids, A7, 1760-1765.
- [5] ISHII M. & ZUBER N. (1979), "Drag coefficient and relative velocity in bubbly, droplet or particulate flows", A.I.Ch.E. Journal, 25, 843-855.
- [6] LILLY, D.K., (1992), "A proposed modification of the Germano subgrid-scale closure method", Physics of Fluids, A4, 633-635.
- [7] NICENO, B., DHOTRE, M.T., SMITH, B.L. (2008), "One-equation sub-grid scale (SGS) modelling for Euler-Euler Large Eddy Simulation (EELES) of dispersed bubbly flow", Chemical Engineering Science, 63, 3923-3931.
- [8] POPE, S.B., *Turbulent Flows*. 2000: Cambridge University Press.
- [9] SMAGORINSKY, J., (1963), "General circulation experiments with the primitive equations: 1. The basic experiment", Monthly Weather Review, 99-164.
- [10] TABIB M.V., ROY S.A. & JOSHI, J.B., (2008), "CFD simulation of bubble column—an analysis of interphase forces and turbulence models", Chemical Engineering Journal, 139, 589-614.
- [11] ZHANG, Y., YANG, C., MAO, Z., (2008), "Large eddy simulation of the gas-liquid flow in a stirred tank", AIChE Journal, 54 (8), 1963-1974.